Supplement Information

Highly homogeneous core-shell Au@Ag nanoparticles with embedded internal standard fabrication by microreactor for reliable quantitative SERS detection

Suyang Li[a||], Junjie Chen[b||], Wanbing Xu[a], Biao Sun[c], Jiechen Wu[d], Qiang Chen [b†], Pei Liang [a†]

a. College of Metrology and Measurement Engineering, China Jiliang University, 310018, Hangzhou, China.

b. College of Optical and Electronic Technology, China Jiliang University, 310018, Hangzhou, China.

c. School of Electrical and Information Engineering, Tianjin University, 300072, Tianjin, China.

d. Department of Sustainable Development, Environmental Science and Engineering (SEED), KTH Royal Institute of Technology, SE-100 44, Stockholm, Sweden.

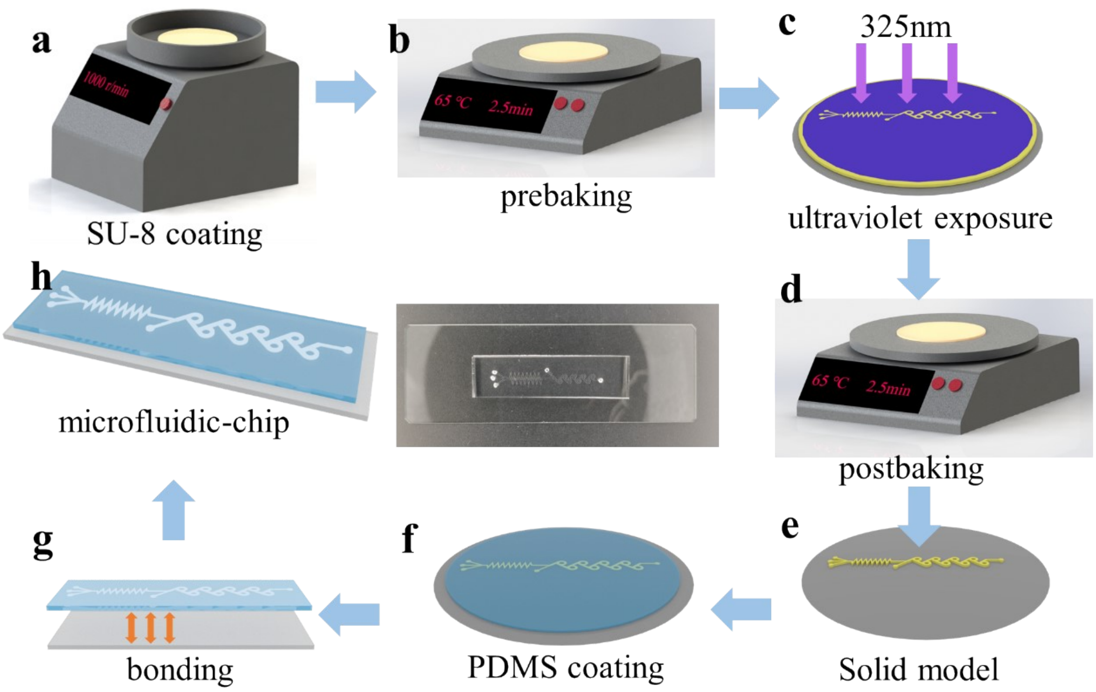

Figure. S1. Method for manufacturing microfluidic-chip (a-h).

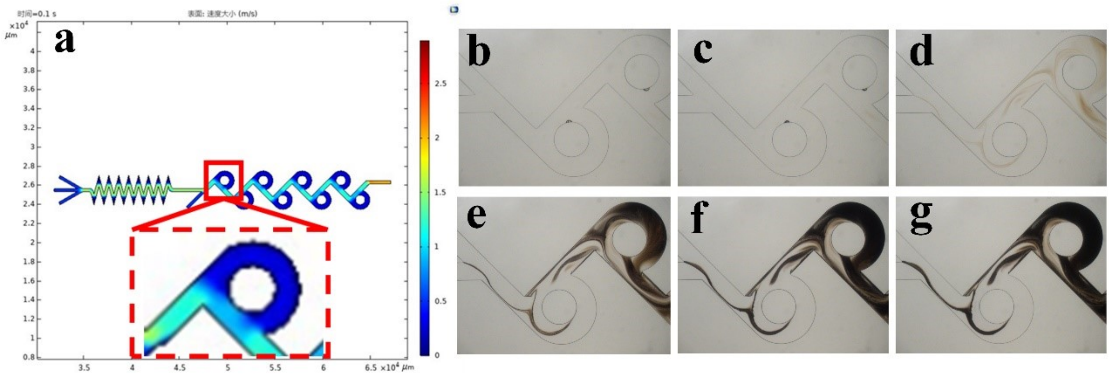

Figure.S2. Flow velocity simulation diagram of microfluidic reactor (a); Ring mixing in the microfluidic reactor (b-g represents the reaction of 0s,1s,10s,60s,2min and 2.5min, respectively).

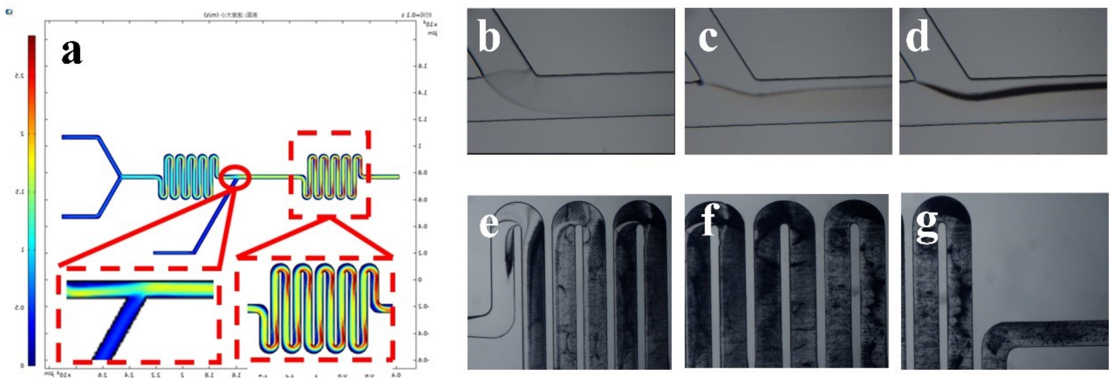

Figure. S3. Flow velocity simulation diagram of S-channel in microfluidic reactor (a); Actual synthesis of microfluidic reactor: fluid junction (b-d stands for 0, 1 and 10s, respectively), S-channel mixing (e-g).

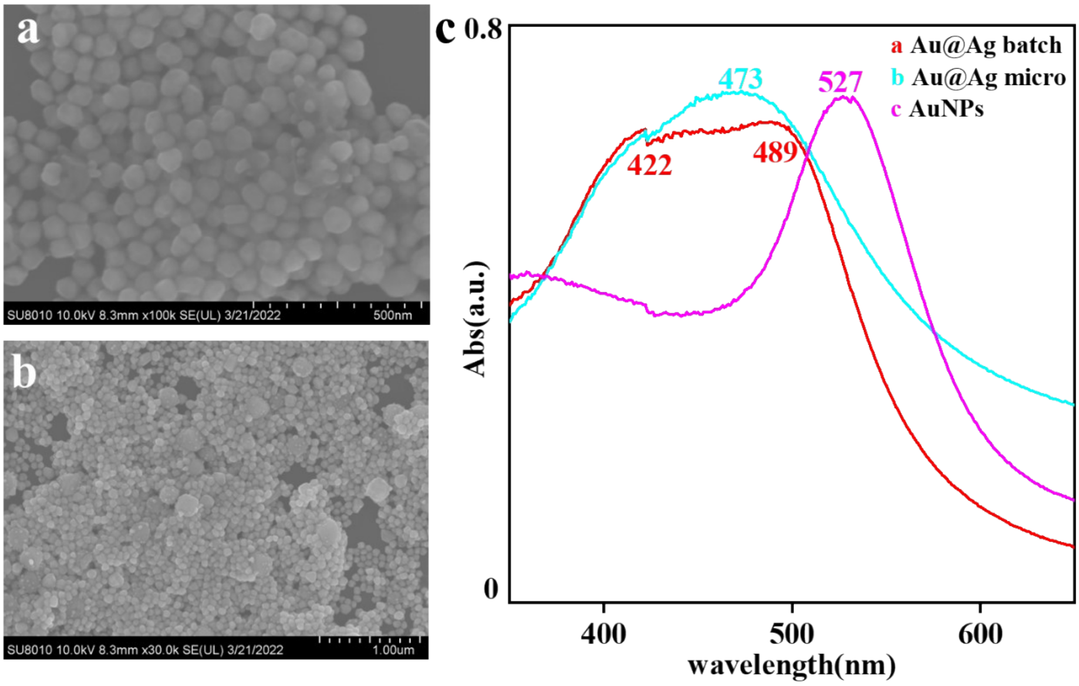

Fig. S4. The SEM images of gold and silver core shells were synthesized by beaker batch. Uv-vis spectra of core-shell nanoparticle solutions obtained by microfluidic and batch synthesis of gold sol and Au@Au, respectively.

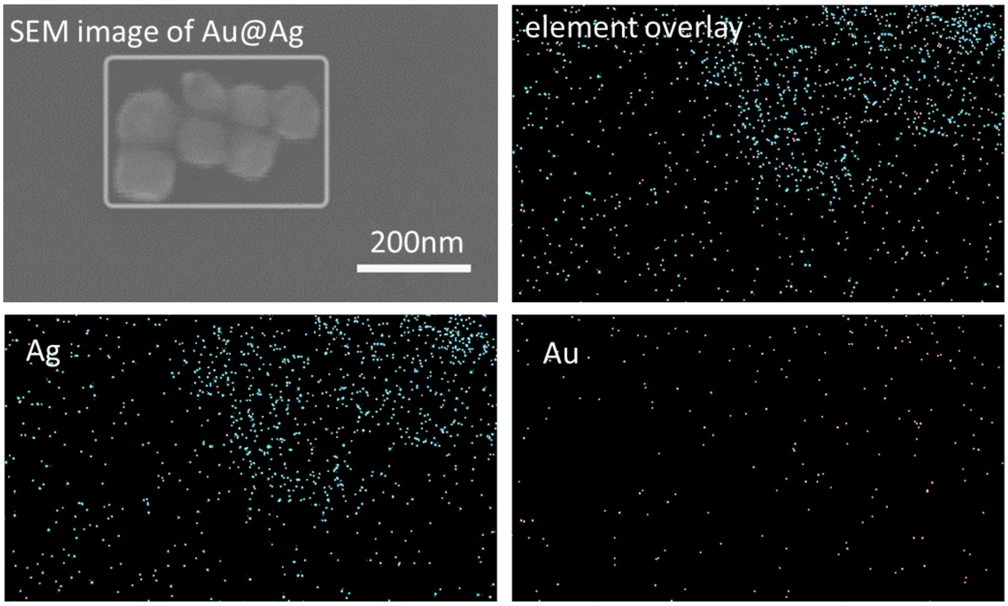

Fig. S5. Typical EDS element diagram Au@Ag core-shell nanoparticles for microfluidic synthesis

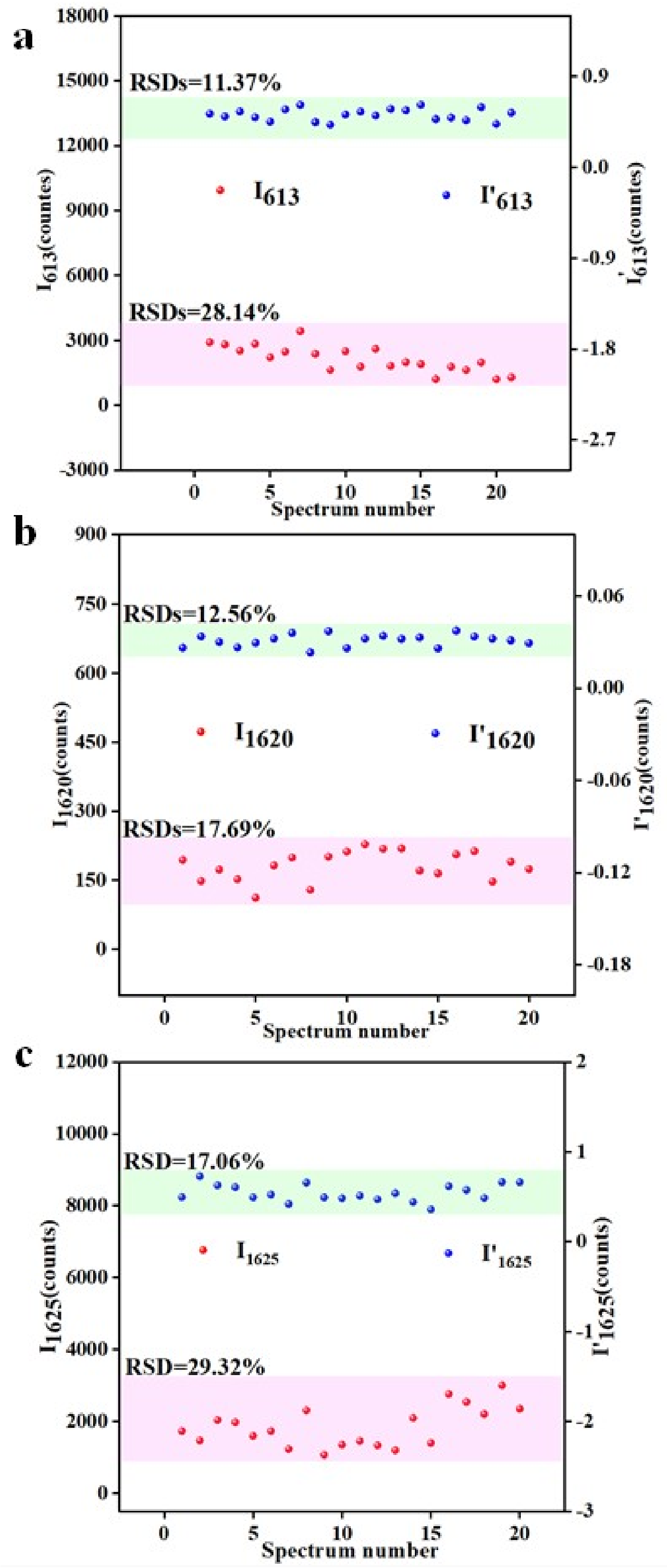

Fig. S6. The random 20 SERS signal distributions from R6G(a)、CV(b)、MB(c) (10^{-6}M) of Au@DTNB@Ag.

Correlation coefficient R^2

In this paper, we use R^2 as a coefficient to measure the linear relationship between the concentration C and the Raman peak intensity of the sample, and the formula for the measurement coefficient R^2 is expressed as follows:

$$R^2 = \frac{\sum_{i=1}^{n}(\hat{S}_i - \bar{S})^2}{\sum_{i=1}^{n}(S_i - \bar{S})^2} = 1 - \frac{\sum_{i=1}^{n}(S_i - \hat{S}_i)^2}{\sum_{i=1}^{n}(\hat{S}_i - \bar{S})^2} \quad \text{……………………………………………………(S1)}$$

where $\sum_{i=1}^{n}(S_i - \bar{S})^2$ is sum of squares for total, $\sum_{i=1}^{n}(\hat{S}_i - \bar{S})^2$ is regression sum of squares, and $\sum_{i=1}^{n}(S_i - \hat{S}_i)^2$ is residual sum of squares.

Table. S1. SERS analysis of R6G、CV and MB in Au@DTNB@Ag core-molecule-shell substrate.

Analyte	Raman intensity	Relationship	LOD(M)
R6G	I_{613}	LogY=7500.92+773.86LogC	$1*10^{-8}$
		R^2 = 0.903	
	I_{613}/I_{1335}	LogY=0.8452+0.0919LogC	
		R^2 = 0.972	
CV	I_{1620}	LogY=9843.99+1605.51LogC	$1*10^{-7}$
		R^2 = 0.973	
	I_{1620}/I_{1335}	LogY=1.7790+0.2942LogC	
		R^2 = 0.994	
MB	I_{1625}	LogY=29343.46+4155.16LogC	$1*10^{-8}$
		R^2 = 0.933	
	I_{1625}/I_{1335}	LogY=7.0245+0.9908LogC	
		R^2 = 0.994	

Table S2 Assignments of Raman bands of R6G in SERS and normal Raman conditions.

Raman	SERS	Assignment
1649	1651	xanthene ring stretch;C-H in-plane bending
1573	1577	xanthene ring stretch;N-H in-plane bending
1502	1512	xanthene ring stretch;C-N stretch;C-H bend;N-H bend
1362	1364	xanthene ring stretch; C-H in-plane bending
1304	1312	xanthene ring breath N-H in-plane bending; CH2 wag
1185	1184	xanthene ring in-plane deformations
773	775	C-H out of plane bend; xanthene ring in-plane deformations

613	613	xanthene ring in-plane deformations; xanthene ring out-of-plane deformations

Table S3 Assignments of Raman bands of MB in SERS and normal Raman conditions.

Raman	SERS	Assignment
1617	1623	(C–C) ring stretching
1597	1395	(C–C) ring stretching
1513	1299	(C–C) antisymmetric stretching
1184	1184	(C–N) stretching
1121	1136	(C–H) out-of-plane bending
670	667	(C–H) out-of-plane bending
612	592	(C–S–C) skeletal deformation
502	498	(C–N–C) skeletal deformation
449	445	(C–N–C) skeletal deformation

Table S4 Assignments of Raman bands of CV in SERS and normal Raman conditions.

Raman	SERS	Assignment
1612	1618	C-phenyl in-plane antisymmetric stretching
1580	1583	C-phenyl in-plane antisymmetric stretching
1530	1530	Phenyl-N antisymmetric stretching
1376	1368	C-N, Phenyl-C-phenyl antisymmetric stretching
1168	1175	C-phenyl, C-H in-plane antisymmetric stretching
908	911	Phenyl ring breathing mode
796	803	Phenyl-H out-of-plane antisymmetric bending
722	728	C-N-C symmetric stretching